

The potential energy of a ^{40}K Fermi gas in the BCS-BEC crossover

J. T. Stewart,* J. P. Gaebler, C. A. Regal, and D. S. Jin

*JILA, Quantum Physics Division, National Institute of Standards and Technology and Department of Physics,
University of Colorado, Boulder, CO 80309-0440, USA*

(Dated: December 2, 2024)

We present a measurement of the potential energy of an ultracold trapped gas of ^{40}K atoms in the BCS-BEC crossover and investigate the temperature dependence of this energy at unitarity. In particular we study the ratio of the potential energy of the gas at unitarity to that of a non-interacting gas, and in the $T = 0$ limit we extract the universal many-body parameter β . We find $\beta = -0.54^{+0.05}_{-0.12}$; this value is consistent with previous measurements using ^6Li atoms and also with recent theory and Monte Carlo calculations. This result demonstrates the universality of ultracold Fermi gases in the strongly interacting regime.

With the emergence of novel Fermi gas systems experimentalists can now access the Bardeen Cooper Schrieffer (BCS)- Bose-Einstein Condensate (BEC) crossover in ultracold gases of atoms. Using atomic scattering resonances in gases of ^{40}K and ^6Li it is possible to widely tune the interatomic scattering length, a , and move continuously between a gas of weakly interacting fermions and a gas of condensed molecules. The BCS-BEC crossover occurs in the strongly interacting regime where the scattering length is large enough that $-1 \lesssim 1/k_F a \lesssim 1$, where k_F is the Fermi wave vector. Experimental studies of these strongly interacting Fermi systems have revealed many interesting properties including a phase transition involving condensates of atom pairs [1, 2], a pairing gap [3], and vortices in a rotating gas [4].

As a gas of fermions is cooled from the classical regime to quantum degeneracy the Pauli exclusion principle becomes manifest in the properties of the ultracold gas [5, 6]. For example, a zero-temperature Fermi gas in a confining potential has a finite energy and a finite size due to Fermi pressure, which is responsible for the stability of white dwarf and neutron stars. In this paper we will address what happens to the potential energy of a trapped gas as the two-body scattering length is tuned to be arbitrarily attractive. One would expect that the gas should be compressed due to attractive interactions and pairing effects [7, 8]; here, we report on the strength to which these effects compress a harmonically trapped Fermi gas and reduce its potential energy.

This behavior has received theoretical consideration and should not depend on the details of the interatomic potential for a wide Feshbach resonance, where the Fermi energy is much smaller than the energy equivalent width of the resonance [9, 10, 11, 12]. Furthermore at unitarity, which is the point where the two-body scattering length a diverges, the energy of the gas is expected to be universal [13, 14, 15] in that it depends only on the Fermi energy E_F and the relative temperature T/T_F . The density profile of a trapped $T = 0$ unitary gas is then expected to be simply a rescaled version of the non-interacting density profile. This results in a simple rescaling of the size and energy, which can be parameterized by a universal

many-body parameter β [16, 17].

Experimentally the size and energy of a trapped ^6Li Fermi gas has been examined [8, 16, 18, 19, 20, 21, 22], and the kinetic energy of a trapped ^{40}K Fermi gas has been measured [23, 24]. The parameter β has been reported only for the case of ^6Li , with the most precise determination, $\beta = -0.54 \pm 0.05$, reported recently in Ref. [21]. While this value is in good agreement with the predicted value, a measurement using a different atomic species is essential to demonstrate the universality of strongly interacting Fermi gases, a topic that has been under debate [10, 12, 25, 26]. Here we report on a measurement of the potential energy at unitarity for an ultracold gas of ^{40}K . We have also measured the potential energy throughout the strongly interacting regime and investigated the temperature dependence of the potential energy at unitarity.

For these experiments we cool a gas of fermionic ^{40}K atoms to ultracold temperatures using previously described methods [23]. A nearly equal mixture of the two lowest energy hyperfine spin states, $|f, m_f\rangle = |9/2, -9/2\rangle$ and $|9/2, -7/2\rangle$, is confined in a crossed beam optical dipole trap. Approximately 10^5 atoms per spin state are cooled to a final temperature of $T \approx 0.08 T_F$, where $T_F = E_F/k_b$ is the Fermi temperature and k_b is Boltzmann's constant. The trap consists of a horizontal laser beam parallel to \hat{z} with a $\frac{1}{e^2}$ radius of $32 \mu\text{m}$ and a vertical beam parallel to \hat{y} with a $\frac{1}{e^2}$ radius of $200 \mu\text{m}$. For the experiments reported here the harmonic trap frequencies were typically $\omega_r/2\pi = 184 \text{ Hz}$ and $\omega_z/2\pi = 18 \text{ Hz}$.

The final evaporative cooling of the gas occurs on the BCS side of the magnetic-field Feshbach resonance where $a \approx -1000 a_0$. The optical trap is then ramped up approximately 1.5 times of the shallowest trap depth used for evaporation to ensure harmonic confinement. To vary a the magnetic field is adiabatically ramped to various final values. The optical trap is then suddenly switched off and the gas is allowed to expand for 1.867 ms . During this short expansion time there is significant expansion in the radial direction but negligible expansion of the cloud in the axial direction. We then use absorption imaging to probe the density distribution of the atom cloud. The

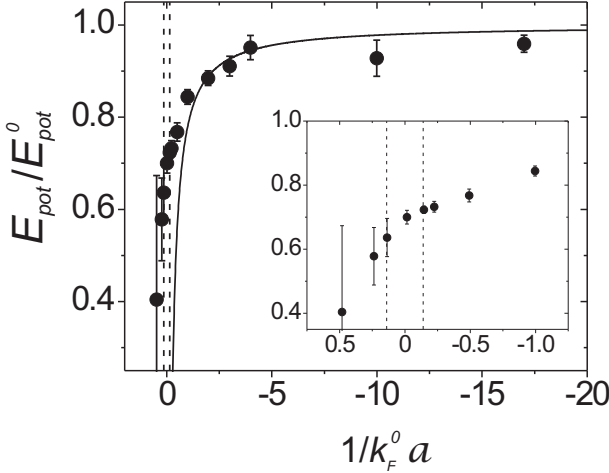


FIG. 1: Measured potential energy E_{pot} normalized to the value measured in the non-interacting regime E_{pot}^0 versus $1/k_F^0 a$. Here $(^0)$ denotes a quantity measured in the non-interacting regime, i.e., at the zero crossing of the s-wave scattering length. The resonance is located at 202.10 ± 0.07 G; the dashed lines show the uncertainty in the resonance location. Data points toward the BEC limit show good agreement with a zero temperature mean-field calculation (solid line). The larger error bars on the BEC side of the resonance reflect uncertainties due to heating of the gas due to inelastic loss. (inset) Subset of the data focusing on the strongly interacting region near resonance.

probe beam propagates along one of the radial directions \hat{x} and is pulsed on for $40 \mu\text{s}$. We obtain the potential energy of the trapped gas from the measured axial density distribution. For each absorption image we perform a 2D surface fit to a finite temperature Fermi-Dirac function

$$OD(y, z) = pk g_2 \left(-\zeta e^{-\frac{y^2}{2\sigma_y^2} - \frac{z^2}{2\sigma_z^2}} \right) / g_2(-\zeta) \quad (1)$$

where ζ , σ_y , σ_z , and pk are independent fitting parameters and $g_n(x) = \sum_{k=1}^{\infty} \frac{x^k}{k^n}$. This is the expected optical depth (OD) distribution for a non-interacting cloud both in trap and after expansion. Empirically we find that this function also fits well in the strongly interacting regime. The potential energy of the trapped gas is obtained from the cloud profile in the axial direction. The potential energy per particle in the axial direction (\hat{z}) is given by

$$E_{pot} = \frac{1}{2} m \omega_z^2 \sigma_z^2 \frac{g_4(-\zeta)}{g_3(-\zeta)} \quad (2)$$

where m is the mass of ^{40}K .

It is useful to consider the ratio of the measured potential energy of the strongly interacting gas to that of an ideal (non-interacting) Fermi gas. For previous experiments done using ^6Li atoms the measured cloud sizes

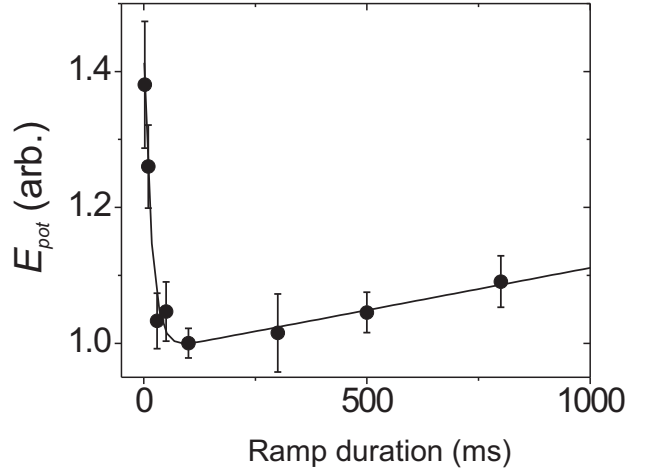


FIG. 2: Measured potential energy at unitarity versus magnetic-field ramp duration. For very fast ramps we measure a higher energy because of nonadiabaticity. For very slow ramps heating due to inelastic collisions increases the measured energy.

and energies were normalized to a calculated value for the non-interacting gas. However for the ^{40}K Feshbach resonance we are able to directly measure the potential energy of the non-interacting gas by going to the zero crossing of the resonance where $a = 0$. Taking this ratio of measurements reduces the systematic uncertainty. The measured potential energy ratio for an ultracold ^{40}K gas is displayed in Fig. 1 as a function of $1/k_F^0 a$. In this paper we use a superscript naught $(^0)$ to denote measurements in the non-interacting regime. The inset to Fig. 1 focuses on the strongly interacting region near the resonance. k_F has a systematic error due to the approximate 50% systematic number uncertainty. As expected, the data show that the interactions cause a strong reduction in the potential energy due to a compression of the trapped gas. One would expect that on the BEC side of the resonance E_{pot} will depend on condensate fraction; for conditions similar to these experiments we find a condensate fraction of approximately 15% [1].

The error bars in Fig. 1 include statistical uncertainty in repeated measurements as well as an uncertainty due to heating during the magnetic-field ramps. The magnetic-field ramps must be sufficiently slow to be adiabatic; however, heating during the ramp can be a problem for slower ramps. For the different final magnetic fields we investigated the dependence of the measured potential energy on the duration of the linear ramp. An example of this is shown in Fig. 2 where the gas was ramped from the magnetic field used for evaporation (203.39 ± 0.01 G) to unitarity.

To determine the optimum ramp rate, as well as the

effect of heating on the potential energy measurement, we fit data such as that shown in Fig. 2 to an exponential decay plus linear heating. From the fit we determine the final potential energy of the cloud if heating were not present. This introduces a correction that is applied to the data shown in Fig. 1. Note that on the BCS side of the resonance we see little or no heating due to magnetic-field ramps, and the error bars are dominated by shot-to-shot statistical uncertainty.

We can gain some theoretical insight into the effect of interactions on the energy of our trapped gas by considering a simple mean-field approach. While this approach neglects pairing and therefore is not sufficient to fully understand the behavior of our gas, it provides a flavor of how the potential energy is affected by interactions. Following the argument outlined in Ref. [17], the equation of state for an ideal zero-temperature Fermi gas is

$$\mu = \epsilon_F(\mathbf{x}) + U_{MF}(\mathbf{x}) + U_{trap}(\mathbf{x}), \quad (3)$$

where μ is the chemical potential, $\epsilon_F(\mathbf{x})$ is the local Fermi energy, $U_{MF}(\mathbf{x})$ is the mean-field contribution, and $U_{trap}(\mathbf{x})$ is the trapping potential. We can relate $\epsilon_F(\mathbf{x}) = \frac{\hbar^2}{2m} k_F^2(\mathbf{x})$ to the density $n(\mathbf{x}) = \frac{1}{6\pi^2} k_F^3(\mathbf{x})$ via $\epsilon_F(\mathbf{x}) = \frac{\hbar^2}{2m} [6\pi^2 n(\mathbf{x})]^{2/3}$. The interactions appear in the density dependent mean-field contribution, $U_{MF}(\mathbf{x}) = \frac{4\pi\hbar^2 a}{m} n(\mathbf{x})$. This equation can be solved self-consistently to determine the in-trap density profile of the cloud, and thus the potential energy per atom. In Fig. 1 we compare the data to the mean-field calculation (solid line) for the normal state on the BCS-side of the resonance [23]. Near the resonance, in the strongly interacting regime, it is clear that this approximation breaks down and a more sophisticated theory is required.

Very near the resonance the scattering length a diverges and the equation given above for $U_{MF}(\mathbf{x})$ becomes unphysical. At unitarity ($1/k_F a = 0$) the only energy scale is the Fermi energy; this give us an approximate effective scattering length $a_{eff} = -1/k_F$. This substitution shows that the local mean-field energy is proportional to the Fermi energy, and one can define a constant of proportionality β given by $U_{MF}(\mathbf{x}) = \beta \epsilon_F(\mathbf{x})$ [8, 16]. In this simple mean-field estimate, $U_{MF}(\mathbf{x}) = -\frac{4}{3\pi} \epsilon_F(\mathbf{x})$, or $\beta_{MF} = -0.41$. The negative sign for the scattering length is not obvious from this approach, but a more sophisticated many-body approach shows the mean-field interaction should be attractive [13]. Now we can write Eq. (3) as

$$\mu = (1 + \beta) \epsilon_F(\mathbf{x}) + U_{trap}(\mathbf{x}). \quad (4)$$

Solving for the density profile for a harmonic trap and then integrating to find the energy per particle, one finds that the potential energy of a $T = 0$ gas at unitarity is simply $E_{pot} = \frac{3}{8} \mu$, just as in the case of a non-interacting Fermi gas. To find the ratio of the chemical potential at

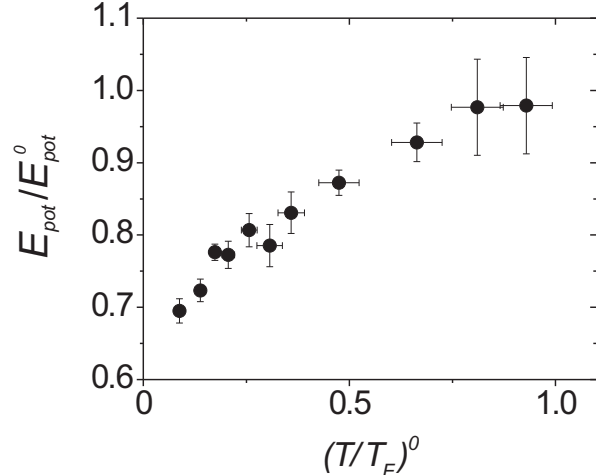


FIG. 3: Potential energy E_{pot} normalized to the measured energy in the non-interacting regime E_{pot}^0 vs the non-interacting gas temperature $(T/T_F)^0$. The cloud is heated by parametrically modulating the trapping potential. For these data the trapping frequencies in the radial direction vary from ~ 180 Hz to 450 Hz and in the axial direction ~ 18 Hz to 21 Hz.

unitarity μ to that for a non-interacting gas μ^0 , we hold the number constant for each case, $N = \int n^0(x) d^3x = \int n(x) d^3x$, to find

$$\frac{\mu}{\mu^0} = \sqrt{1 + \beta}. \quad (5)$$

Thus, the universal parameter β can be extracted by measuring the ratio of the potential energy at unitarity to the potential energy of a non-interacting Fermi gas, in the $T = 0$ limit.

From the data in Fig. 1 we find $E/E_0 = 0.70 \pm 0.02$ on resonance giving $\beta^* = -0.51 \pm 0.03$. Whereas β is normally only defined for $T = 0$ we introduce $(*)$ to denote that the system is at a finite temperature $(T/T_F)^0 = 0.08 \pm 0.01$. This experiment was conducted at $202.20(\pm 0.01)$ G and the error bars include statistical error as well as the heating effects mentioned above. Including uncertainty in the resonance position we find $\beta^* = -0.51^{+0.04}_{-0.12}$.

We now consider experimentally the question of whether the gas is sufficiently cold to be in the $T = 0$ limit as required for an accurate determination of β . In Fig. 3 we show the measured potential energy ratio as a function of $(T/T_F)^0$. In this experiment we heat the gas by parametrically modulating the optical trap strength. However, before heating the gas we first increase the optical trap depth to prevent number loss and ensure harmonic confinement. Both the resulting temperature $(T/T_F)^0$ and k_F^0 are determined using an ultracold cloud prepared as described above and slowly ramping the mag-

netic field to the point where $a = 0$ just before the trap is turned off. The gas is allowed to expand freely for 14 ms and fit according to Eq. (1). We extract $(T/T_F)^0$ from the fugacity ζ of the non-interacting cloud using $g_2(-\zeta) = -(T/T_F)^{-3}/6$. It is important to note that in this experiment we expect the magnetic field ramps to keep the entropy constant but not the temperature.

The data in Fig. 3 clearly show that the universal many-body parameter β depends strongly on temperature. Furthermore, it is not clear that a gas at $(T/T_F)^0 = 0.08$ is sufficiently cold to determine the $T = 0$ limit of β . For the purpose of extrapolating to zero temperature we fit a quadratic function to the data points below $(T/T_F)^0 = 0.25$ for which we find $\beta = -0.54^{+0.05}_{-0.11}$. The error bars reflect the uncertainty in the extrapolation to $T = 0$ and the uncertainty in the resonance position. This value of the universal many-body parameter β , as well as the value at $(T/T_F)^0 = 0.08$, is in good agreement with Monte Carlo calculations [27, 28, 29, 30, 31] and a recent theoretical calculation of $\beta = -0.545$ in Ref. [32]. These values are also in good agreement with multiple experimental reports in ${}^6\text{Li}$: $\beta = -0.73^{+0.12}_{-0.09}$, -0.61 ± 0.15 , -0.49 , and -0.54 ± 0.05 in Refs. [19], [20], [22], and [21] respectively. We also note that from the kinetic energy measurement in ${}^{40}\text{K}$ reported in Ref. [23] we can extract $\beta = -0.62 \pm 0.07$ [33]. This is in good agreement with the value of β found using the potential energy presented in this paper.

In summary we have studied the potential energy of a strongly interacting quantum degenerate Fermi gas of ${}^{40}\text{K}$ atoms. At unitarity our results are consistent with current theory as well as previous experiments in ${}^6\text{Li}$. These results provide strong evidence that the ${}^{40}\text{K}$ and ${}^6\text{Li}$ Fermi gas systems are universal. We have also measured the temperature dependence of a universal many-body parameter that could be compared to recent Monte Carlo results for the temperature dependent energy of a homogeneous Fermi gas, reported in Refs. [31, 34].

We thank the JILA BEC group for stimulating discussions. This work was supported by the NSF, NIST, and NASA; C. A. R. acknowledges support from the Hertz Foundation.

- [3] C. Chin *et al.*, *Science* **305**, 1128 (2004).
- [4] M. W. Zwierlein, J. R. Abo-Shaeer, A. Schirotzek, C. H. Schunck, and W. Ketterle, *Nature* **435**, 1047 (2005).
- [5] B. DeMarco and D. S. Jin, *Science* **285**, 1703 (1999).
- [6] A. G. Truscott, K. E. Strecker, W. I. McAlexander, G. B. Partridge, and R. G. Hulet, *Science* **291**, 2570 (2001).
- [7] H. T. C. Stoof, M. Houbiers, C. A. Sackett, and R. G. Hulet, *Phys. Rev. Lett.* **76**, 10 (1996).
- [8] M. E. Gehm, S. L. Hemmer, S. R. Granade, K. M. O'Hara, and J. E. Thomas, *Phys. Rev. A* **68**, 011401(R) (2003).
- [9] R. B. Diener and T.-L. Ho, cond-mat/0405174 (unpublished).
- [10] R. B. Diener and T.-L. Ho, cond-mat/0404517 (unpublished).
- [11] S. Simonucci, P. Pieri, and G. C. Strinati, *Europhys. Lett.* **69**, 713 (2005).
- [12] M. H. Szymanska, K. Goral, T. Kohler, and K. Burnett, *Phys. Rev. A* **72**, 013610 (2005).
- [13] H. Heiselberg, *Phys. Rev. A* **63**, 043606 (2001).
- [14] G. A. Baker, *Phys. Rev. C* **60**, 054311 (1999).
- [15] T.-L. Ho, *Phys. Rev. Lett.* **92**, 090402 (2004).
- [16] K. M. O'Hara, S. L. Hemmer, M. E. Gehm, S. R. Granade, and J. E. Thomas, *Science* **298**, 2179 (2002).
- [17] C. Menotti, P. Pedri, and S. Stringari, *Phys. Rev. Lett.* **89**, 250402 (2002).
- [18] T. Bourdel *et al.*, *Phys. Rev. Lett.* **91**, 020402 (2003).
- [19] M. Bartenstein *et al.*, *Phys. Rev. Lett.* **92**, 120401 (2004).
- [20] T. Bourdel *et al.*, *Phys. Rev. Lett.* **93**, 050401 (2004).
- [21] G. B. Partridge, W. Li, R. I. Kamar, Y. an Liao, and R. G. Hulet, *Science* **311**, 503 (2005).
- [22] J. Kinast *et al.*, *Science* **307**, 1296 (2005).
- [23] C. A. Regal, M. Greiner, S. Giorgini, M. Holland, and D. S. Jin, *Phys. Rev. Lett.* **95**, 250404 (2005).
- [24] Q. Chen, C. A. Regal, D. S. Jin, and K. Levin, cond-mat/0604469 (unpublished).
- [25] M. Mackie and J. Piilo, *Phys. Rev. Lett.* **94**, 060403 (2005).
- [26] J. Javanainen, M. Kostrun, M. Mackie, and A. Carmichael, *Phys. Rev. Lett.* **95**, 110408 (2005).
- [27] J. Carlson, S. Y. Chang, V. R. Pandharipande, and K. E. Schmidt, *Phys. Rev. Lett.* **91**, 050401 (2003).
- [28] J. Carlson and S. Reddy, *Phys. Rev. Lett.* **95**, 060401 (2005).
- [29] G. E. Astrakharchik, J. Boronat, J. Casulleras, and S. Giorgini, *Phys. Rev. Lett.* **93**, 200404 (2004).
- [30] G. E. Astrakharchik, J. Boronat, J. Casulleras, and S. Giorgini, *Phys. Rev. Lett.* **95**, 230405 (2005).
- [31] E. Burovski, N. Prokof'ev, B. Svistunov, and M. Troyer, *Phys. Rev. Lett.* **96**, 160402 (2006).
- [32] A. Perali, P. Pieri, and G. C. Strinati, *Phys. Rev. Lett.* **93**, 100404 (2004).
- [33] From the kinetic energy one would expect $E_{kin}/E_{kin}^0 = \frac{3-2\beta}{3\sqrt{1+\beta}}$.
- [34] A. Bulgac, J. E. Drut, and P. Magierski, *Phys. Rev. Lett.* **96**, 090404 (2006).

* Electronic address: J.Stewart@jila.colorado.edu; URL: <http://jilawww.colorado.edu/~jin/>

- [1] C. A. Regal, M. Greiner, and D. S. Jin, *Phys. Rev. Lett.* **92**, 040403 (2004).
- [2] M. W. Zwierlein *et al.*, *Phys. Rev. Lett.* **92**, 120403 (2004).